

# Severe rockburst occurrence during construction of a complex hydroelectric plant

G. Russo

Geodata Engineering (GDE), Corso Bolzano 14, Turin, Italy

**ABSTRACT:** Severe rockbursts occurred during the construction of a complex hydroelectric plant in the Andean region of Chile, causing severe support failures and prohibitive work conditions. Consequently, a technical solution had to be found and fundamental safety issues achieved by completely automated support installation. A very accurate seismic monitoring was implemented, permitting the collection of basic information for understanding the seismic events associated with the rockbursts. Although extremely severe rockburst occurrences persisted, also in relation to the high natural seismicity, the close collaboration among Owner, Contractor and Designer allowed for a satisfactory damage control using effective support systems.

## 1 INTRODUCTION

This paper deals with the technical solution for controlling severe rockburst occurrence during the on-going construction of a complex hydroelectric plant in a seismic Andean region of Chile.

After a general setting of both the observed brittle instability phenomena, involving heavy failure of the previous installed support (Section 2) and geomechanical conditions (Section 3), the rationale and the dimensioning of new mitigation measures are described (Section 4). Brief insight into the adopted numerical model is presented in Section 5.

The effective performance of the new support system is analyzed in Section 6 in relation to successive severe rockburst occurrences.

## 2 GENERAL OVERVIEW

The intensity and frequency of seismic events dramatically increased while excavating one of the access tunnels to a powerhouse, just after a lithological contact between pyroclastic tuff and andesitic lava of the Abanico Western Formation (Oligocene-Miocene) with about 800 m of overburden (Figure 1).

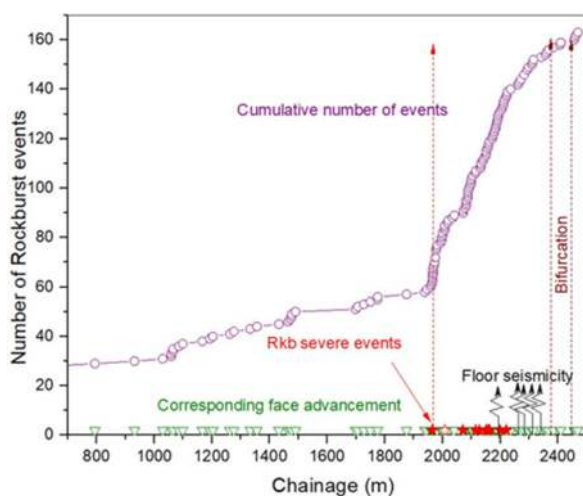


Figure 1. Cumulative number of rockburst events in access tunnel. Red dotted line coincides with lithological contact, while arrow indicate the first severe rockburst.



Figure 2: Initial modification of the excavation shape by Contractor to follow the failure mode (7.35 m of vertical dimension)

After the first severe event reported in the Figure 1, a progressively increasing tendency to overbreaks and rock block ejection was observed in the tunnel (Figure 2).

Measures for controlling the dangerous brittle instabilities included modifications to the excavation shape (Figure 2) and adding a joint in the shotcrete in tunnel crown with the purpose of reducing stress concentrations (see Figure 3). The support system was based on two (1.5m x 1.5m) sequences of rock reinforcement (L=3m) by PM16/24 Swellex and Shell Anchored bolts (d=25mm) alternated with D-Bolts (22mm), in combination with (70+50mm) Fiber Reinforced Shotcrete (FRS) and two 6mm weld-meshes (ACMA C188).

These technical solutions were however not able to control the damage from a very violent rockburst event that occurred at about Chainage (pk) 2+070 (overburden  $\approx$  930m), resulting in severe support failures at about 10m from the tunnel face followed by further support damage up to about 30m from the face (Figure 3).

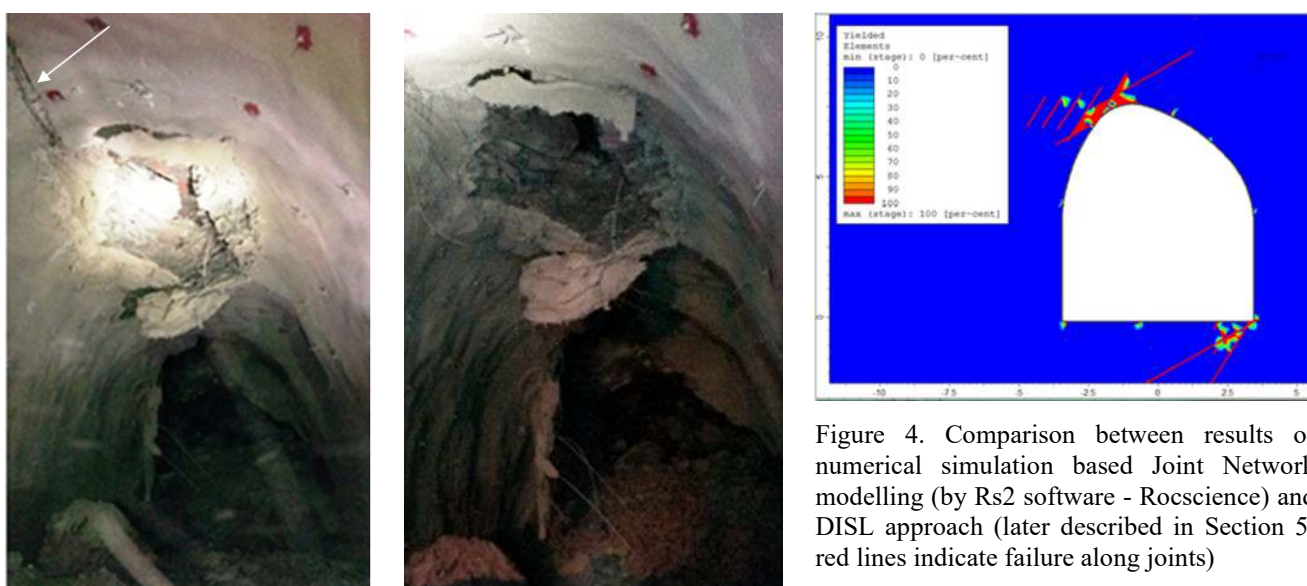


Figure 3. Support damage by severe rockburst at pk 2+070 (the arrow indicates the joint in the shotcrete).

In Figure 4, the result of a numerical simulation is compared with observed collapse, showing a satisfactory agreement between expected/observed failure localization and extension.

Kaiser and Cai (2013, 2018) classify this type of rockburst as “*strainbursts*”, i.e. a sudden and violent failure of rock near an excavation boundary caused by excessive straining of a volume of stiff and strong rock (burst volume). If triggered by a face burst, the secondary seismic source is co-located at the damage location. If self-initiated, the primary seismic source is located at the damage location.

On the other hand, some uncertainty still exists concerning the further sub-classification proposed by the cited authors, also in relation to successive events registered during the construction of other tunnels and caverns in the same hydroelectric project. In particular, although probably the “*Self-initiated/Mining-induced*” resulted as the most frequent strainburst type, it cannot be excluded that, depending on the augmented intensity of eventual remote seismic events induced by excavation, also “*seismically triggered*” or even “*dynamically loaded*” strainburst occurred.

In dynamically loaded strainburst the energy radiated from a primary source impacts in two possible forms:

- (i) it causes a dynamic stress pulse that may deepen the depth of failure, thus releasing more stored energy and, through rock mass bulking, adding strain or displacement to the rock and support; or
- (ii) it transfers some of its radiated energy to kinetic energy and assists in ejecting marginally stable rock.

In the former case, according to the Canadian Rockburst Support Handbook (CRSH, 1996) the maximum dynamic stress increment that needs to be added to the tangential stress, temporarily modifying the Stress Level  $SL = \sigma_{max}/UCS$  (i.e. the ratio of the max tangential stress on excavation contour to the intact rock strength) and increasing the depth of failure, is:

$$\Delta\sigma^d_{max} = \pm 4 \cdot c_s \cdot \rho \cdot PGV_s \quad \text{where: } c_s = \text{propagation speed of shear waves; } \rho = \text{density of rock mass}$$

PGVs= Peak (particle) Ground Velocity of the shear waves which depends on the seismic event magnitude and distance from the source.

### 3 GEOMECHANICAL CONDITIONS

According to the available information, based on both CSIRO and Hydraulic fracturing in situ tests, the main regional principal stress is oriented between NE-SW and E-W, with a ratio of major horizontal to vertical stresses  $k = (\sigma_H/\sigma_V) \sim 2 \div 2.5$ . Moreover, generally  $\sigma_V$  results higher than the minor horizontal stress ( $\sigma_h$ ), thus indicating remarking a typical "strike-slip" condition.

In the so-called "GDE multiple graphs" of Figure 5 (Russo, 2014), the main geomechanical properties (GSI, UCS,  $IC = \sigma_{cm}/\sigma_{tang(max)}$  and RMR) from about Chainage pk 1900m onwards in the access tunnel are shown in combination with the expected excavation hazards (quadrant IV) for the relative plane-strain principal stresses.

As it can be observed from this figure by proceeding clockwise from the bottom-right to the top-right to the top-left quadrant (I→IV; see basic equations rationale reported outside the graph):

- I quadrant (bottom-right): in the case not implemented for GSI assessment
- II quadrant (bottom-left):  $GSI \approx 47 \div 66$ ;  $UCS \approx 150 \div 200 \text{ MPa}$
- III quadrant (top-left):  $IC \approx 0.05 \div 0.2$
- IV quadrant (top-right):  $RMR \approx 50 \div 65$ . Consequently, in terms of excavation behaviour, serious overbreaks conditions, eventually associated to severe rockburst, are expected in alternative to rock wedges instability.

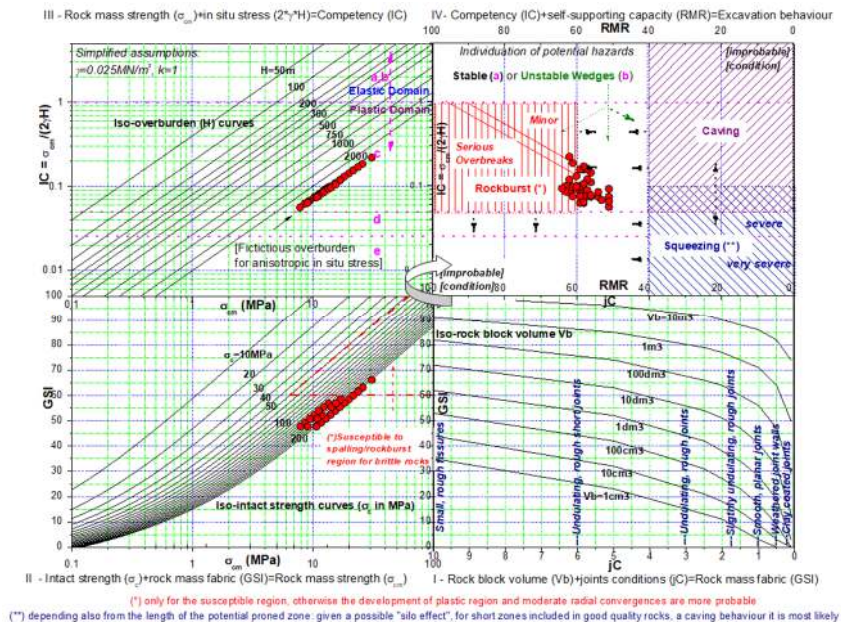


Figure 5. Application of the GDE Multiple graphs (Russo, 2014) for the 1+900÷2+070 Adit stretch. Note that "fictitious" overburden in top-left quadrant allows for considering the effective max tangential stress ( $3\sigma_1 - \sigma_3$ ) related to  $k \neq 1$ .

The assessment of rockburst hazard through the the GDE multiple graph refers to the spalling classification proposed by Diederichs et al., (2010; Figure 6), based on the empirical prediction of the depth of brittle failure as a function of the stress level  $SL = \sigma_{max}/UCS$  (Wiseman, 1979, reported in CRSH, 1996; Martin et al., 1999). In Figure 7, the Stress Level (SL) is detailed for an Adit stretch with reference to the increasing overburden and the localization of rockburst events.

In Figure 8, the Dynamic Rupture Potential (DRP, Diederichs, 2017) is estimated for the same UCS range reported in Figure 5, by consequently remarking an indication of possible rock ejection in case of unsupported or ineffectively supported excavations. As suggested by Stacey (2016), ejection velocity could even be much higher than indicated in the graph and velocity in the order of 10m/s are not uncommon, thus adding uncertainty to design.

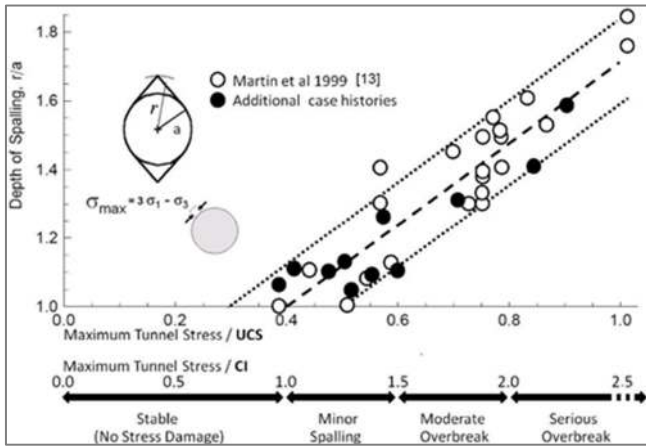


Figure 6. Empirical prediction of Depth of Spalling/Failure=DoF) for  $SL < 1$ . The figure (Diederichs et al., 2010) is based on CRSH (1996) and Martin et al., (1999).  $CI = \text{Crack Initiation Threshold} = 0.4 \cdot UCS$  in the graph. According to Nicksiar and Martin (2013),  $CI = 0.35 \div 0.55$  for most of rocks. The cases in figure remark the maximum registered DoF, generally for brittle failures (no rockburst).

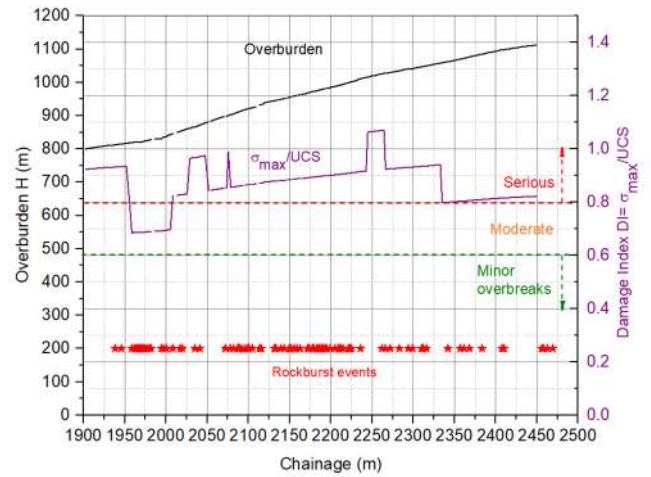


Figure 7: Relation between rockburst events and the calculated Stress Level. Note that the SL drops after Chainage pk 2+320 was hypothesized due to increases in UCS derived from laboratory tests.

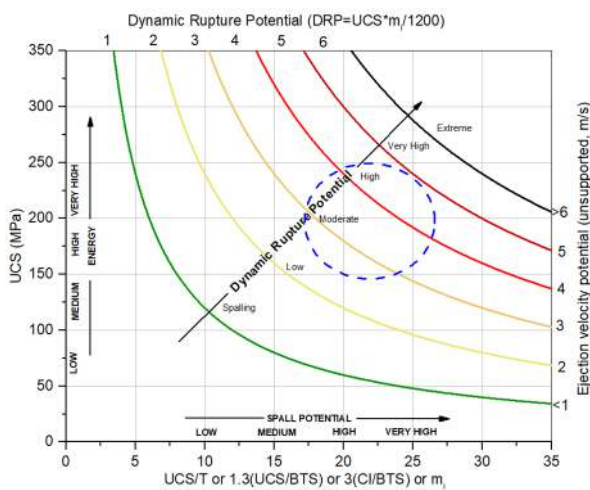


Figure 8: Dynamic Rupture Potential (DRP) for massive rock (Diederichs, 2017) with approximate indication of typical Andesitic Lavas properties

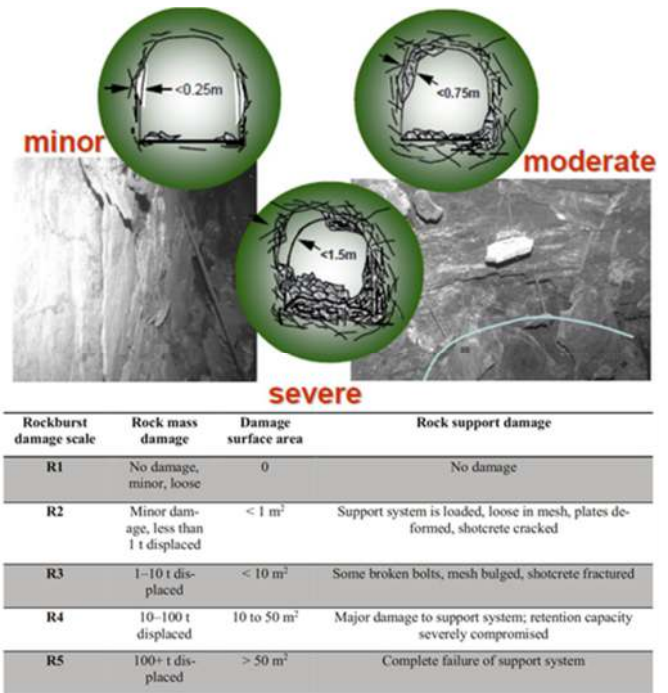


Figure 9: Above: Classification of rockburst damage severity for unsupported excavations (Kaiser et al., 1996). Below: Rockburst damage scale for support (Potvin, 2009; modified by Cai and Kaiser, 2018)

According to Cai and Kaiser (2018), the brittleness indices in Figure 8 in the horizontal axis are indicators of StrainBurst Potential (SBP) and on the vertical axis of StrainBurst Severity (SBS). The UCS contributes to the severity of events, but other factors, particularly the “Relative Brittleness”, related to the excavation system stiffness (Tarasov and Potvin, 2013) need to be considered.

For unsupported tunnel (width and height dimension in the range of 3÷6m) Kaiser et al. (1996) defined the rockburst damage severity in terms of depth of failure as shown in the upper part of Figure 9. At the bottom of the same figure, the rockburst damage scale for support (Potvin, 2009, modified by Cai and Kaiser, 2018) is reproduced.

#### 4 UPGRADED DESIGN SOLUTION

The extremely dangerous conditions remarked by the rockburst event at Chainage pk 2+070 imposed a substantial revision of the applied mitigation measures and in 2016 the Contractor involved Geodata Engineering (GDE) for devising an adequate and safe technical solution.

Safety conditions for the workers, by avoiding any exposure in potentially dangerous zone, is the fundamental requisite for design in rockburst environment. In line with this basic requirement, the Contractor provided special bolting equipment for the automated installation of steel mesh and bolts.

At the same time, an accurate seismic monitoring system was deemed of paramount importance.

The design dimensioning development basically followed the approach described by Kaiser et al. (CRSH, 1996), with basic reference to "Bulking causing ejection" as the dominant damage mechanism.

Depending on the possible interaction between the different elements of the support system and relative failure occurrences, it was estimated that the described rockburst event at pk 2+070 (Figures 3-4) released energy at least for 20 kJ/m<sup>2</sup> and up to about 30 kJ/m<sup>2</sup>. Therefore, the latter was considered the reference energy demand for rockburst design.

How to consider in rockburst design the contribution of the reinforcement and surface support in the overall system is still debated. According to Potvin et al. (2010, 2013), the surface support (shotcrete, steel mesh) could theoretically guarantee an additional safety margin but actually it often just represents the "weakest link" that will work in a "serial" function with reinforcement/holding system.

Additionally, Cala et al. (2013) remarked a variable redistribution of the energy in the different support elements as a function of the relative stiffness of the surface component. For example, according to the tests performed by Villaescusa and Player (2015) on composite support (bolt and steel mesh), the reinforcement adsorbed about 72 to 93% of the released energy.

Considering the uncertainty on the effective interaction between holding/reinforcement and retention system, the weakest link issue and the potential ejection velocity, a double-layer solution was consequently dimensioned, as shown in Figure 10.

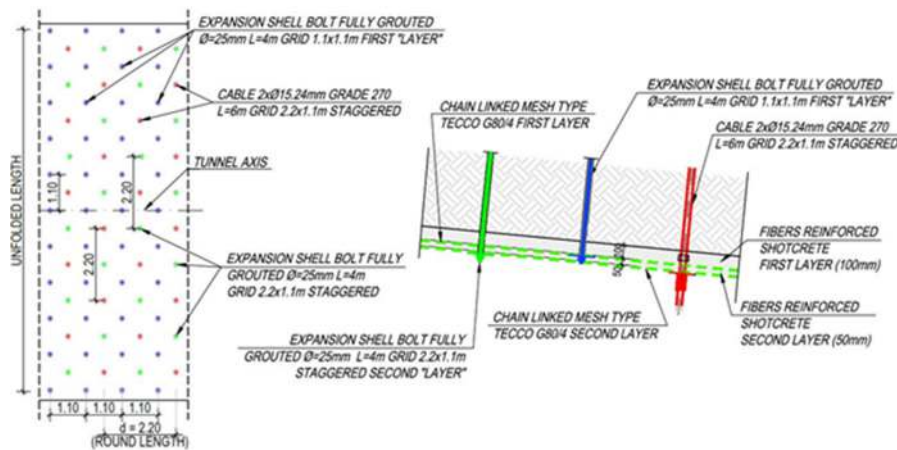


Figure 10: Double-layer solution dimensioned for severe rockburst occurrence

The double-layer solution (crown/sidewalls) typically involves two retention system components: Fibre-Reinforced Shotcrete (FRS) and high capacity chain-linked steel mesh (Tecco G80/4). Each component was combined with a radial reinforcement by fully grouted 25mm expansion shell threadbars or twin-(15.2mm) strand cables. The latter served as partial alternative holding elements for the second retention component, depending on excavation cross section.

Based on available results from tests on bolts and retention systems (in particular by the WASM Dynamic Test Facility, as reported by Villaescusa et al., (2015), CANMET, (2012) and *drop test* data reported by Potvin et al., (2010), including Kaiser et al. (1996) and Ortlepp and Stacey, (1997)), the reinforcement/holding system is called to adsorb in about 100-(150) mm of displacement the energy demand of reference with a Factor of Safety  $FS \approx 2$ , as recommended by CRSH. At the same time, the retention component guarantees a capacity itself in the order of demand, offering by the chain-link mesh component some further deformational margin.

Furthermore, as a measure for some controlled dissipation of seismic energy, a curved excavation shape was used for the invert and by temporarily leaving at the face the blasted rock, in order that invert zone results filled up to the horizontal working plane. The standard technical solution also included the retention and reinforcement of the tunnel face by FRS+welded mesh and PM24 Swellex bolts. Forepoling was applied in particular critical stretches to further control overbreak.

A representative image of the application of the Double-layer solution is presented in Figure 11.



Figure 11: Examples of application of the Double-layer solution and tunnel face control

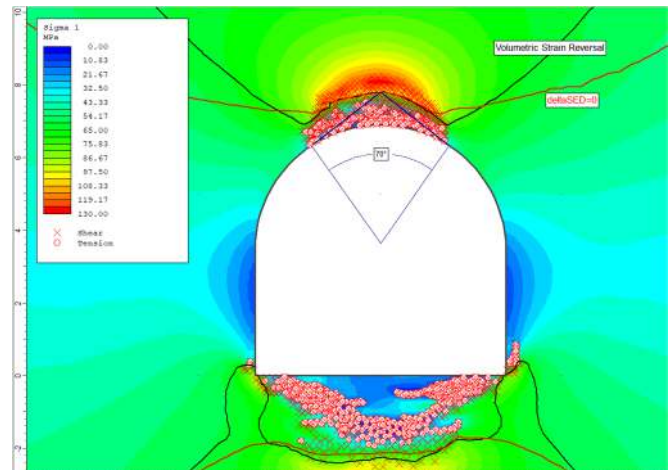


Figure 12. Example of results of numerical modelling by Rs2 in terms of major stress (Sigma1) and yielding zones. VSR and the iso-line  $\Delta SED=0$ , as well as the potential brittle failure notch according to Martin et al. (1999) are additionally remarked.

## 5 INSIGHT FROM NUMERICAL MODELLING

Numerical analyses were conducted with the main purpose of understanding the potential localization of brittle failure and the extension of the stress-damage zone around the cavity.

The DISL (Damage Initiation Spalling Limit) approach (Diederichs, 2010) based on the multi-phase failure criterion was adopted.

In Figure 12, the results of an example of implementation of DISL by continuum are provided in terms of major stress (Sigma1) and yielding zone (x for shear and o for tension). Moreover, the following additional elements are highlighted:

- The Volumetric Strain Reversal (VSR): according to Perras and Diederichs (2016), VSR indicates the transition between isolated and connected damage within the rock mass surrounding the excavation and should be comparable to the depth of brittle failure investigated by Martin et al., (1999, Figure 6). Consistent with this reference, the approximate dimension of the potential brittle failure notch is as well reproduced.

- An approximate indication of the limit between zones in which Strain Energy Density (SED) reduced (close excavation) or increased in the passage from elastic peak to post-failure condition. Therefore, this limit is remarked by the union of points in which SED did not change, i.e. the iso-line  $\Delta SED = SED_{\text{post-failure}} - SED_{\text{peak}} = 0$ . The Strain Energy Density is calculated by the following formula:

$SED=[(\sigma_1^2+\sigma_2^2+\sigma_3^2)-2\nu(\sigma_1\sigma_2+\sigma_2\sigma_3+\sigma_3\sigma_1)]/2E$  where:  $\sigma_1,\sigma_2,\sigma_3$ = Principal Stresses;  $\nu$ =Poisson Ratio;  $E$ =Young Modulus.

It can be observed that VSR and  $\Delta SED=0$  overlaps in the tunnel crown, so consistently estimating the potential thickness of unstable rock mass. Numerical model does not give the maximum (extreme) DoF as per Figure 6.

Based on the resulting VSR and the associated Depth of Failure (DoF), an estimate of the kinetic energy ( $E_k$ ) can be assessed. For the example in Figure 12, considering DoF~1m and the potential ejection velocity derived from Figure 8, the previously remarked energy demand for design is approximately confirmed.

## 6 PERFORMANCE OF SUPPORT SYSTEM

The application of the technical solution for severe rockburst was extended to all the tunnels and caverns exposed to such a critical hazard, with some optimization depending on local geomechanical conditions, as for the dominance of tuff in place of andesitic lavas. Here, probably in relation to both lower UCS and higher CI, frequency and severity of rockburst generally show some reduction. Violent brittle failures persisted in all excavation in andesitic lithologies, as for example illustrated in Figure 13 for the zone around the powerhouse. In Figure 14, the time of occurrence of rockburst after blasting is related to the relative distance from the tunnel face. Most rockbursts occurred within 24 hours and at less than 5H distance (i.e. ~37 m) from the face (H=Height of excavation section). Only three events occurred at 40÷80 m from the face.



Figure 13. Rockburst locations and damage severity in the zone of the Powerhouse

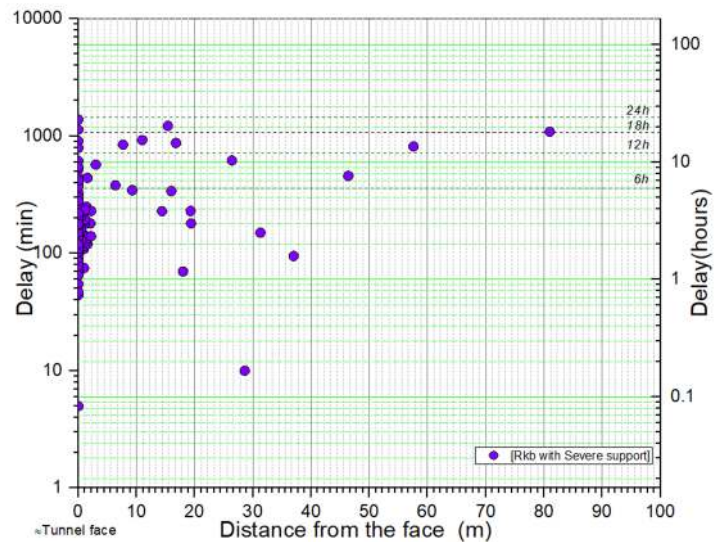


Figure 14: Time of occurrence (Delay) of rockburst after blasting vs relative Distance from the face

The performance of the double-layer solution has been satisfactory. The support system was able to control very violent events by limiting the damages, without critical structural failure.

In occasion of the most severe events, the following type of damages have been observed (Figure 15):

- Fracturing of the shotcrete along preferred alignment, without fall-down or ejection of fragments because of the chain-link mesh protection;
- local shear cut of the threadbars. This kind of failure prevalently occurred at distance <0.5m from the bolt heads (no twin-strand cables shear failures).
- cracks in the invert zone, sometimes consequence to very impressive up-down movement of the floor, like earthquake shaking associated to seismic waves propagation (see also Figure 1).

With reference to the table in Figure 9, the R3 grade of the scale can be assessed, but observing that the associated damage surface area is much more than indicated in the classification system.

Due to the support damage, part of the support system capacity has been consumed and it is necessary to estimate the remnant capacity of the support system. Consequently, after a cautious removal of the failed elements, the support capacity can be restored by stepwise integrative measures (see Kaiser, 2013 and Cai and Kaiser, 2018). As anticipated, a key element of the upgraded design agreed with Owner and Contractor was the implementation of a seismic monitoring system. An extremely high seismicity has been observed as resulting from the D&B (Drill and Blast) tunnel advancements: in several occasions more than 10,000 seismic events per week were registered, with some hundred events with moment magnitude  $M_w > -1$  and maximum values up to  $M_w = 1.4$  (see details in Russo G., 2019).



Figure 15. Examples of damage of the support systems in crown and invert for severe rockburst events

## 7 CONCLUSIVE REMARKS

Rockburst probably poses the most dangerous and many times unpredictable hazard affecting underground excavation in highly stressed hard/massive rocks. This paper describes a very demanding technical challenge to control this kind of phenomenon during construction at depth of a complex hydroelectric scheme in a seismic active region.

After several attempts to implement different mitigation measures as suggested in the literature, which however could not prevent severe failures to the support system from taking place, a substantial change in construction approach in terms of equipment and technical solution had to be adopted.

In particular, given the absolute priority given to safety, automated bolters for a complete mechanized installation of support elements were introduced so as to avoid any exposure of workers.

An innovative compatible double-layer solution for reinforcement and retention system was dimensioned to achieve an adequate safety margin with respect to the rockburst energy and displacement demand.

The technical solution was then implemented at all underground excavation exposed to similar hazards. This support performed satisfactorily by limiting the support damages despite many severe rockburst occurrences in very high stress conditions.

Seismic monitoring performed a fundamental role for a comprehensive analysis and understanding of these complex and hazardous phenomena.

*ACKNOWLEDGMENT: The author wishes to acknowledge the much-appreciated contributions of his colleagues Simone Addotto, Carlo Chiesa and Domenico Parisi.*

## REFERENCES

- Cai M. and Kaiser P.K. 2018: Rockburst Support Reference Book. Available to download from: [http://www.imseismology.org/imsdownloadsapp/webresources/filedownload/Cai-Kaiser\(2018\)-Rockburst-Support-Voll.pdf](http://www.imseismology.org/imsdownloadsapp/webresources/filedownload/Cai-Kaiser(2018)-Rockburst-Support-Voll.pdf)
- Cala M., Roth A. & Roduner A., 2013: Large scale field tests of rock bolts and high-tensile steel wire mesh subjected to dynamic loading. *Rock Mechanics for Resources, Energy and Environment* Edited by Marek Kwaśniewski and Dariusz Łydźba.
- CAMIRO Mining Division, 1996. *Canadian Rockburst Research Handbook (CRSH)*.
- Diederichs, MS, Carter, T. Martin. 2010. *Practical Rock Spall Prediction in Tunnel*. Proc. of World Tunnelling Congress. Vancouver.
- Diederichs, M.S. 2017. *Early Assessment of Dynamic Rupture and Rockburst Hazard Potential in Deep Tunneling*. SAIMM 2017 in Capetown (Afrirrock)
- Hoek, E. and Martin CD, 2014. *Fracture initiation and propagation in intact rock - A review*. *Journal of Rock Mechanics and Geotechnical Engineering*
- ISRM, 2015 Xiao et al.: *Suggested Method for In Situ Microseismic Monitoring of the Fracturing Process in Rock Masses*, 2015
- Kaiser, P.K. and Kim B.H., 2008: *Rock Mechanics Advances for Underground Construction in Civil Engineering and Mining*. Keynote Rock Mechanics Symposium. Seul.
- Kaiser, P.K. and Cai M., 2013: *Critical review of design principles for rock support in burst-prone ground-Time to rethink! Perth - Seventh International Symposium on Ground Support in Mining and Underground Construction*. Perth
- Kaiser P.K. 2017: *Ground control in strainburst ground –A critical review and path forward on design principles*. 9th Inter. Symposium on Rockburst and Seismicity in Mines (Santiago, Chile)
- Li C.C., 2010. *A new energy-absorbing bolt for rock support in high stress rock masses*. *International Journal of Rock Mechanics & Mining Sciences* 47. 396–404.
- Martin C.D., Kaiser P.K, and McCreath D.R., 1999. *Hoek–Brown parameters for predicting the depth of brittle failure a round tunnels*. *Canadian Geotechnical Journal*. 36: 136–151.
- Ortlepp, W.D. and Stacey, T.R., 1997. *Testing of tunnel support: dynamic load testing of rock support containment systems*, SIMRAC GAP Project 221.
- Perras M. and Diederichs M.S. 2016. *Predicting excavation damage zone depths in brittle rocks*. *Journal of Rock Mechanics and Geotechnical Engineering*. 8, pp 60-74
- Player J.R., Morton E.C., Thompson A.G. and Villaescusa E. (2008): "Static and dynamic testing of steel wire mesh for mining applications of rock surface support". SAIMM, SANIRE and ISRM: 6th International Symposium on Ground Support in Mining and Civil Engineering Construction
- Potvin Y., Wasseloo J. and Heal D., 2010. *An interpretation of ground support capacity submitted to dynamic loading Deep Mining 2010 — M. Van Sint Jan and Y. Potvin (eds) © 2010 Australian Centre for Geomechanics, Perth, ISBN 978-0-9806154-5-6*.
- Potvin Y and Wasseloo J. 2013. *Towards an understanding of dynamic demand on ground support*. *The Journal of The Southern African Institute of Mining and Metallurgy*, n.113.
- Russo G. 2014. *An update of the "multiple graph" approach for the preliminary assessment of the excavation behaviour in rock tunneling*. *Tunnelling an Underground Space Technology* n.41.
- Russo G. 2018: *Rockburst*. Lecture for Post Graduated Master Course "Tunnelling and Tunnel Boring Machines" - Politecnico di Torino - Academic Year 2017-2018 ([https:// www.geodata.it/giordandue/](https://www.geodata.it/giordandue/))
- Russo G. 2019. "Severe rockburst occurrence during construction of a complex hydroelectric plant". Lecture for the 29th Mine Seismology Seminar- IMS Institute of Mine Seismology 05-07 May 2019 – Phoenix, Arizona (USA) ([https:// www.geodata.it/giordandue/](https://www.geodata.it/giordandue/)).
- Stacey T.R. and Ortlepp W.D., 2001. *Tunnel surface support capacities of various types of wire mesh and shotcrete under dynamic loading*. *The Journal of The South African Institute of Mining and Metallurgy*.
- Stacey T.R., 2016. *Addressing the Consequences of Dynamic Rock Failure in Underground Excavations* *Rock Mech. Rock Eng.* DOI 10.1007/s00603-016-0922-3
- Tarasov B. and Potvin Y. 2013. *Universal criteria for rock brittleness estimation under triaxial compression*. *International Journal of Rock Mechanics & Mining Sciences* n.59.
- Villaescusa E. and Player J.R. 2015. *Dynamic Testing of Ground Support Systems*. MRIWA Report n.312.